Microdomain Morphology of Star Copolymers in the Strong-Segregation Limit

David M. Anderson and Edwin L. Thomas*

Department of Polymer Science and Engineering, University of Massachusetts, Amherst, Massachusetts 01003. *Received February 2, 1988; Revised Manuscript Received March 30, 1988*

ABSTRACT: The strong-segregation limit of microphase separation in *star* diblock copolymers is treated with a mean-field theory originally introduced for linear diblocks by Leibler and extended for the strong segregation limit by Ohta and Kawasaki. In addition to the usual morphologies of spheres, cylinders, and lamellae, the ordered bicontinuous double-diamond (OBDD) structure discovered in experiments in our group is included in the free energy competition. The structure factor for a star copolymer is that derived by de la Cruz and Sanchez, and the long-range contribution to the free energy is computed by a numerical summation over reciprocal lattice vectors. Constant-mean-curvature surfaces with double-diamond symmetry, calculated by a finite element method, are used to define model OBDD structures, and the form factors for the model structures so defined are calculated analytically. These constant-mean-curvature surfaces yield lower free energies than either surfaces determined by assemblies of cylindrical struts or surfaces displaced a constant distance from the Schwarz "diamond" minimal surface. The conclusion that the constant-mean-curvature surface is the best description of the microscopic interface is also supported by comparisons of calculated projections with actual TEM data. Use of these surfaces of constant mean curvature is thus crucial in proper modeling of the OBDD morphology. The predicted lattice parameters for the OBDD structures observed in the star diblocks for arm numbers above five by Thomas and co-workers and in the linear diblocks by Hashimoto and co-workers are in very good agreement with experiment, but the calculated free energy of the OBDD morphology does not become less than that of the cylindrical morphology in either the star or linear diblock cases as is indicated by the experiments. This is most likely due to the inadequacy of Gaussian chain statistics in the microphase-separated state—particularly with respect to the higher arm stars.

Introduction

Until very recently, attempts to fabricate polymeric materials that hybridize the best properties of two or more component polymers have been limited by the tendency for dissimilar polymers to phase-segregate either macroscopically (blends) or into morphologies in which one phase is discrete (block copolymers). Fetters and co-workers initiated the synthesis of a new class of *star* diblock copolymers.[1] A star diblock copolymer consists of a number of identical diblock arms linked to a common center, forming a macromolecule with an inner core region rich in one component and an outer region of the second component. A new equilibrium morphology has been discovered[2,3] in star diblock copolymers which has the property that both phases are continuously connected in all three dimensions. In this so-called "ordered bicontinuous double-diamond" (OBDD) morphology, one phase (e.g., polystyrene) resides in two intertwined but distinct labyrinthine networks that each exhibit diamond-cubic symmetry, and the other phase (e.g., polyisoprene) resides in the continuous matrix between the two diamond channels. This matrix is bisected by a connected, triply periodic surface named the "Schwarz diamond minimal surface";[4] a minimal surface is by definition a surface with identically zero mean curvature (the possibility of bicontinuous morphologies in fluid microstructures was first pointed out by Scriven[5]). The potential importance of a triply periodic, bicontinuous morphology in microcomposites is illustrated by the 10-fold increase in the storage modulus over that of the cylindrical morphology at the same composition but different arm number.[3,6]

The double-diamond morphology occurs for star diblock PI/PS copolymers with a volume fraction of 0.27 for the outer PS blocks, at higher arm numbers; for example, at an arm molecular weight of 33 000, the OBDD occurs for arm numbers of six or more, up to 18, the highest arm number investigated. The range of PS volume fraction over which the OBDD morphology is found is estimated to be 0.27–0.32, for 18-arm stars.[7] The OBDD is also found when the roles of PI and PS are reversed, that is, 30 wt % PI outer blocks.[7] The same morphology has been recently proposed as an equilibrium morphology in high-MW PS-PI linear diblocks.[8] Kinning et al.[9] also observed the OBDD in a sample of a lower MW PS/PW linear diblock.

The theory of microphase separation in block copolymers has seen significant advances in recent years, particularly since the introduction by Leibler[10] of a mean-field thermodynamic potential calculated with the use of a random phase approximation. Leibler's theory for the weak-segregation limit of a linear diblock was recently adapted to the strong-segregation limit by Ohta and Kawasaki[11] and extended by Fredrickson and Helfand[12] to include fluctuation effects. Star diblock and simple graft copolymers were treated in the weak-segregation limit in a theory similar to Leibler's by de la Cruz and Sanchez.[13] The latter authors pointed out that in order to correctly treat the strong-segregation limit of star diblock copolymers, the new OBDD morphology would have to be included in the treatment.

The theory of Ohta and Kawasaki for linear diblocks involves a free energy competition between candidate morphologies, which were taken to be cubic-close-packed spheres, hexagonal-packed cylinders, and lamellae. Bicontinuous morphologies were not treated. The regions of stability for these three phases were calculated to be $0 < \phi < \phi_1 = 0.215$ for bcc spheres, $\phi_1 < \phi < \phi_2 = 0.355$ for cylinders, and $\phi_2 < \phi < 0.5$ for lamellae, with symmetric results for $\phi > 0.5$. These results agree at least qualitatively with many experiments on linear diblocks. In order to obtain an analytical solution for these three morphologies, the (inverse of the) static structure factor of a linear diblock was approximated over the full q range by a three-term expression, which matched the RPA expression to 4% accuracy.

In this paper we extend the theory of Ohta and Kawasaki to the case of star diblock copolymers, including in the free energy competition the OBDD morphology and using the expression for the static structure factor of a star diblock derived by de la Cruz and Sanchez, which includes as a special case ($n = 1$) the linear diblock structure factor derived by Leibler and by Ohta and Kawasaki. The calculation involves a summation over reciprocal lattice

0024-9297/88/2221-3221$01.50/0

vectors, where each term in the sum is calculated analytically, and 2000 terms (actually 68 000 counting multiplicities) are summed yielding an accuracy of better than 0.05% for the sum. The inputs to the model are N_0, the number of statistical segmental lengths in an arm; χ, the Flory interaction parameter; and n, the arm number. The lattice parameter predictions are moderately sensitive to the segmental lengths. However, as in previous theories, the dependence on χ is through the product χN_0 of the interaction parameter per monomer times the arm polymer index, which is independent of the characteristic ratio. Thus, ambiguities in definitions of the χ parameter per monomer[14] are minimized. The results of Ohta and Kawasaki are retrieved by taking $n = 1$ in the limit of large N_0, for the case where the segmental lengths and densities are the same for the two polymers (the "symmetric case").

We begin in section 1 with a review of the exact model used for the OBDD structure. The model is determined by an interfacial surface that is a triply periodic surface of constant mean curvature (a surface of constant mean curvature is sometimes called an "H-surface" for short), taken from one of five families of such surfaces calculated by one of the authors[15] using a finite element method. For a given volume fraction and symmetry group, the surface that minimizes surface area must have constant mean curvature. The surface areas of these H-surfaces are in fact approximately 6% lower than those of the cylindrical-strut surfaces, called tetrapod networks by Hasegawa et al.[8] and depicted by Thomas et al.[2] (see Figure 4), at the same volume fractions. The form factors of the morphologies determined by these finite element surfaces are calculated analytically in section 2.

In section 3 the theory is reviewed and the computation described. The long-range contribution to the free energy, in the nomenclature of Ohta and Kawasaki, is computed by a summation over reciprocal lattice vectors, for each periodic structure. The summand is of the product of the squared form factor of the structure, times the inverse of the structure factor for a star diblock copolymer after the subtraction of certain terms that are treated with the short-range contribution. The short-range contribution is calculated following Ohta and Kawasaki as the product of the interfacial area, times an interfacial tension that is taken to be independent of morphology. The minimization over the lattice parameter is done by Newton's method, to yield the total free energy and a prediction for the equilibrium lattice parameter.

In section 4 the results of the theory are compared with the experiments on star diblocks of Alward et al.[3,16] and those of Hasegawa et al.[8] on linear diblocks. Taking the value of the interaction parameter χ for PI/PS determined by Mori et al.[17] yields a comparison with the theory that is free of any adjustable parameters. The agreement between predicted and measured lattice parameters for the star diblocks is very good, but the free energy of the OBDD morphology does not become less than that of the cylindrical morphology at higher arm numbers as is indicated by experiments. Predicted lattice parameters agree well with TEM data of Hasegawa et al. on OBDD morphologies observed in high-MW PI/PS linear diblocks, although again the cylindrical morphology, not the OBDD, is predicted to be the equilibrium morphology at these compositions.

Section 5 is a discussion of the results.

1. The Model OBDD Structure

The family of H-surfaces computed earlier by one of the authors[15] that will be used to define the model OBDD morphology is perhaps easiest to understand in the following terms. Begin with diamond cubic-close-packed spheres of radius R, so that the subvolume C inside the spheres lies in a matrix M, and $\phi_C = 0.3401$. The surface of each sphere is of course a surface of constant mean curvature, where the mean curvature H at a point is defined to be $H = (k_1 + k_2)/2$, k_1 and k_2 being the principal curvatures at the given point. In this paper (as in ref 15), we will use a dimensionless mean curvature H^* defined by $H^* = HX$, the product of the dimensional mean curvature with the lattice parameter. Now imagine joining each sphere to each of its four adjacent neighbors with a small "neck", after first shrinking the spheres slightly to create gaps for these necks. This fusing of the spheres can actually be done in such a way that the new C/M dividing surface is of constant mean curvature, this constant being slightly greater than the mean curvature, $H^* = 8/3^{1/2}$, of the original sphere-pack. This new triply periodic structure has exactly the symmetries of the original space group, $F\bar{4}3m$, but the value of ϕ_C has decreased, the surface area per unit cell S has decreased, and the C regions have connected into a single, continuous, labyrinthine region. We have chosen the letter "C", for "channels", to represent the subvolume lying inside this labyrinthine region, which is threaded by a diamond graph of degree (or coordination number) four.

One can in fact track a family of such structures, where every structure in the family is of space group $F\bar{4}3m$, is topologically equivalent to the bicontinuous structure just described, and is characterized by a continuous dividing surface of constant mean curvature. As shown in Figure 1a, the value of this mean curvature varies with the volume fraction in a surprising way. Equally surprising is the fact (Figure 1b) that the dimensionless surface area per unit cell S/X^2 exhibits a rather dramatic minimum at a volume fraction of approximately $\phi_C = 0.131$. As discussed in ref 15, the value of $S/V^{2/3}$ for a lattice-fundamental region of this surface, which is exhibited with computer graphics in Figure 2, is smaller than for any other known triply periodic H-surface. This is an important feature for the occurrence of the OBDD structure in block copolymers.

The well-known relation of $dS = 2H\,dV$ between the increments in surface area and volume (in this case volume fraction) holds throughout as this family is tracked. Since Figure 1b gives S versus V, the mean curvature is given by one-half the slope of the curve at each point. This relation also implies that the surface corresponding to the minimum in area in this family is also the point of least volume fraction, $\phi_C = 0.131$; this corresponds to the cusp in Figure 1b.

The surface with H identically zero—a "minimal surface"—in this family has an analytical representation that was discovered by Schwarz[4] and has since become known as the Schwarz diamond or "D" surface. This surface, as calculated by the finite element method, is shown in Figure 3. The surface area calculated from the finite element approximation to this surface was within 0.015% of the known analytical value (no figures are available for comparison in the cases with nonzero mean curvature). The group of symmetries for this special member of the family is larger than that for each of the other members, the space group being $Pn3m$. This minimal surface contains infinite straight lines and therefore divides space into two distinct but congruent regions; this is because a rotation of π about a straight line on a minimal surface is a (orientation-reversing) symmetry of the entire surface.

If this same rotation is applied to any other member of the family (in which case the line itself will not lie on the

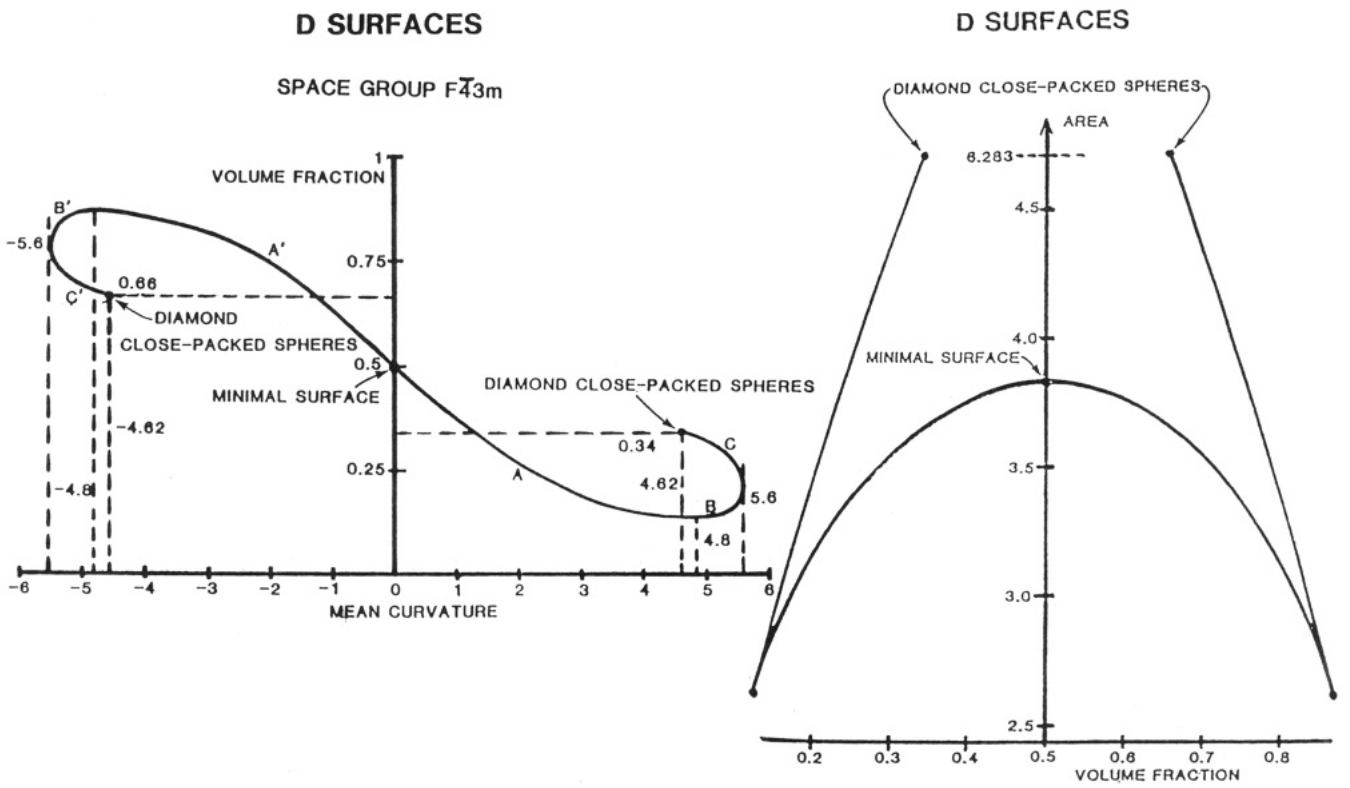

Figure 1. (a, Left) A plot showing the relationship between the dimensionless mean curvature H^* and the channel volume fraction of one of the two subspaces created by the dividing surface of a family of constant-mean-curvature surfaces with $F\bar{4}3m$ or single-diamond symmetry. (b, Right) Relationship between the channel volume fraction and the normalized surface area for dividing surfaces of the single-diamond family. The mean curvature is given at each point by one-half the slope of the curve. For points to the left of the vertical axis, the channel volume fraction of a corresponding double-diamond geometry is obtained by doubling the volume fraction as in (a). As explained in the text, no rescaling of the normalized area is necessary for the double-diamond geometry.

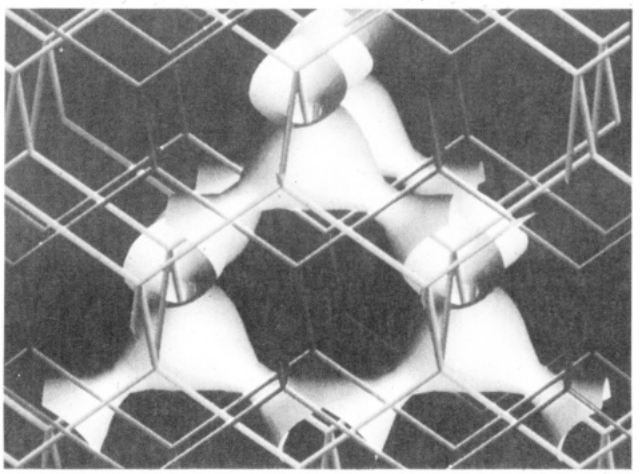

Figure 2. Computer-generated image of a triply periodic surface of constant mean curvature. The surface belongs to a family of surfaces which includes the classical Schwarz *D* minimal surface (see Figure 3). One of the diamond graphs may be surrounded by an identical copy of the surface that surrounds the other graph. The volume fraction inside each of the diamond symmetry channels is 0.131.

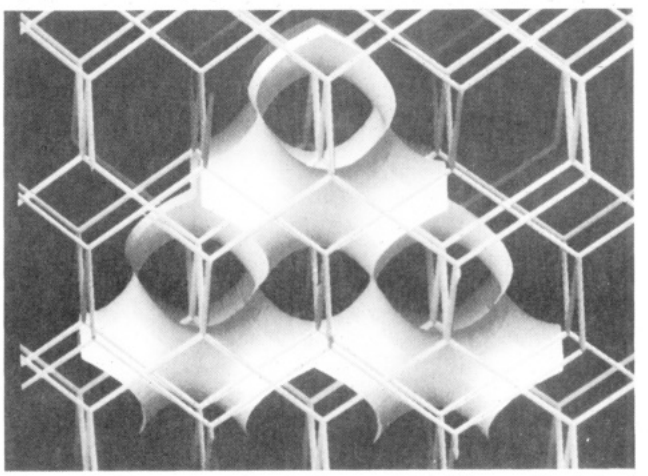

Figure 3. Computer-generated image of the Schwarz *D* minimal surface. This surface subdivides space into two continuous subvolumes of 0.50 volume fraction.

surface), the rotation will not be a symmetry but rather will create an identical copy of the surface which will be displaced from the original by one-half of an $F\bar{4}3m$ unit cell lattice vector (the statement by Thomas et al.[2] that the replica surface is displaced by half a body diagonal is based on this $F\bar{4}3m$ unit cell). The space group of the surface together with this copy is then $Pn3m$, because this rotation is now a symmetry (Schoen[18] discussed the possibility of *H*-surfaces related to the D minimal surface but did not discuss the double-diamond geometry). Furthermore, the minimal surface describes exactly the midplane between the two replicas, in that mirror reflection through the minimal surface takes one replica into the other.

An ordered, bicontinuous, double-diamond structure can then be represented by filling the two diamond networks with material *C* and filling the remaining matrix, which is bisected by the minimal surface, with material *M* (thus *C* and *M* stand both for the regions and the materials occupying them). The space group is $Pn3m$, and the lattice parameter is one-half that of the lattice parameter given above for the single-diamond $F\bar{4}3m$ structure. The effects of a smaller unit cell, rescaling, and the factor of 2 for the double-diamond as opposed to single diamond all cancel out so that the surface area per unit cell is the same as that

Table I[a]
Surface Areas and Free Energies of OBDD Models

		H-surface	parallel surface	cylindrical-strut surface
surf. area		2.983 56	3.017 32	3.174 62
free energy	$n = 1$	1.136 62	1.146 25	1.158 60
	$n = 4$	1.000 13	1.008 58	1.020 58
	$n = 7$	1.004 60	1.013 05	1.025 19

[a] Surface areas and selected free energy data for three models of the OBDD structure. The volume fraction of the outer block is $f = 0.356$ and the parameters used for the calculation of the free energies at the three arm numbers ($n = 1, 4, 7$) indicated are $N_0 = 100$, $\chi = 0.2$, with the segmental lengths and densities of the A and B blocks taken equal. Units of the energy are as in Ohta and Kawasaki.[11]

given in Figure 1b. The largest volume fraction ratio of the two components that can be represented by this family of structures is 0.738:0.262, which occurs at $H^* = 2.4$ (this value of H^* being one-half that in Figure 1a at the minimum, because of the smaller lattice parameter X for the double diamond).

From Figure 1a it is seen that for a given volume fraction ϕ_C between 0.262 and (say) 0.4, there exist two distinct model structures in the family, one with $H^* < 2.4$ and one with $H^* > 2.4$. Figure 1b and the relation $dS = 2H\,dV$ or equivalently $d(S/X^2) = 2H^*\,d\phi_C$ show that the structure with a smaller value of H^* is the structure with the smaller surface area. The total free energies calculated as in section 3 were found to be significantly higher for the surface of higher area at the same volume fraction, so that the model surfaces used were those with $H^* < 2.4$.

Although the H-surfaces minimize surface area under the constraints of volume fraction and of double-diamond symmetry, other shapes for the C/M interface better assimilate the statistics desired by the copolymer chains. Component C is better served by an interface closer to the "cylindrical-strut" model originally depicted in Thomas et al.[2] (see also Hasegawa et al.[8]); this dividing surface lies at a constant distance from the two diamond graphs mentioned above (and shown in Figure 2) which are in any case center lines of the diamond channels. Or component M might desire an interface closer to a surface that is parallel to the minimal surface, the latter surface being in any case the midplane of the M regions. A "parallel" surface is a surface that is the locus of points a constant distance along the normals to a given surface, so named because one can show that the normals at corresponding points are parallel. One can calculate analytically the surface area and volume per unit cell for a surface parallel to the D minimal surface at a distance s, taking $X = 1$:

$$S = S_0 - 8\pi s^2, \qquad \phi_A = S_0 s - 8\pi s^3/3 \tag{1}$$

where S_0 is twice the area of the minimal surface, known in terms of complete elliptical integrals as $S_0 = 2 \times 1.918\,893\,09...$

Starting with the finite element representation of the minimal surface, parallel surfaces at various distances were computed. Also, cylindrical-strut surfaces were computed, all in the same finite element representation. The surface areas at one volume fraction are given in Table I for a typical comparison; as is well-known, the surface of constant mean curvature is the area-minimizing surface (see Nitsche[19] for an in-depth discussion of this theorem). The total free energies (as computed in section 3) for the parallel and cylindrical strut surfaces, for one representative set of parameters, are given in Table I. The surface of constant mean curvature in all cases checked, yielded free energies lower than the other candidate surfaces, by amounts that are significant in view of the small free energy differences involved in the competition between morphologies. We thus conclude that proper modeling of the free energy competition requires the constant-mean-curvature surfaces in the OBDD morphology. This, in turn, virtually rules out an anayltical solution using the correct dividing surface, because the analytical representation of these surfaces is in terms of hyperelliptic integrals.

We have carried out computations of the variation in width of the M regions and find (Anderson et al.[20]) that the root-mean-square deviation of this width is only about 7% of the average width (this width being twice the distance from the minimal surface along its normal to the H-surface). Therefore the parallel surfaces and the H-surfaces at the same volume fraction are almost indistinguishable visually.

2. Form Factor of the OBDD Structure

We now describe the calculation of the form factor of a structure with an interface represented by a finite element surface, whether a constant-mean-curvature, parallel, or cylindrical-strut surface. If the scattering densities on the C and M sides of the dividing surface are taken to be $\Psi = 1 - \phi_C$, and $\Psi = -\phi_C$, respectively (so that $\langle\Psi\rangle = 0$), then the divergence theorem can be used to reduce the volume integration over the unit cell to a surface integral[21]:

$$\int\int\int e^{i\mathbf{q}\cdot\mathbf{r}}\Psi(\mathbf{r})\,d^3\mathbf{r} = (i/q^2)\int\int \mathbf{n}\cdot\mathbf{q}e^{i\mathbf{q}\cdot\mathbf{r}}\,dA \tag{2}$$

This surface integral can be performed analytically over each triangular patch in the finite element representation of the surface. For a space triangle with vertices $\mathbf{r}_1$, $\mathbf{r}_2$, and $\mathbf{r}_3$, this integral is

$$\{[\cos(a+b) - \cos(a+c)]/b(c-b) - [\cos a - \cos(a+c)]/bc\}p/q^2 \tag{3}$$

where $a = \mathbf{r}_1\cdot\mathbf{q}$, $b = \mathbf{r}_2\cdot\mathbf{q} - a$, $c = \mathbf{r}_3\cdot\mathbf{q} - a$, and $p = |(\mathbf{r}_2 - \mathbf{r}_1) \times (\mathbf{r}_3 - \mathbf{r}_1)|$. The form factor calculated at reflections that are forbidden in the $Pn3m$ space group [all ($hk0$) with $h + k$ odd] was in all cases less than 10^{-19}. The form factor calculated for a very small value (0.01) of H^* compared very well with the form factor of the minimal surface computed numerically by Mackay[22] and with that computed in ref 15 by a surface integration. The structure for the case of a very small H^* consists of a very thin shell bisected by the minimal surface. There are no figures available for analytical values of form factors for any of these H-surfaces, for direct comparison. However, the equation just given is an analytical formula for the structure as represented by finite elements, and so the deviations of the finite element solutions from the actual constant-mean-curvature surfaces (surfaces which have recently been given mathematical existence proofs[23]) have only a very small effect on the computed form factor, which is after all a volume integral.

3. Calculation of the Free Energies

We now describe the calculation of the total free energy of a star diblock copolymer in each of the candidate morphologies, using the results of de la Cruz and Sanchez and the approach of Ohta and Kawasaki but with some important modifications of the latter approach. The nomenclature used will be that of Ohta and Kawasaki. The computation will first be described for the case where there is no molecular asymmetry between the A and B segments; that is, the monomer lengths—statistical segmental lengths in actuality—of A and B will be equal and the monomer densities the same. Each (identical) arm of the star will have type A monomers for the contour length $0 < \tau < \hat{f}$ and B monomers for the contour length $\hat{f} < \tau < N_0$, where

n such diblock arms are connected at $\tau = 0$ to form an n-armed star. Thus the convention is that the inner blocks are denoted by A and the outer by B. The total polymer index of the star is nN_0. The volume fraction of A is then $f = \hat{f}/N_0$. The density of monomers is ρ_0, the local deviation of the monomer density is $\hat{\Psi}$, and the density variable used in the calculation will be $\Psi = \hat{\Psi}/\rho_0$ as in the last section; the form factor is then Ψ_q. One should note that the χ of de la Cruz and Sanchez differs from that of Ohta and Kawasaki by a factor of ρ_0, and in this paper we will use the former definition, so that the combination of $\chi\rho_0$ appearing in the formulas of Ohta and Kawasaki will be given by simply χ. The units of this χ are those of energy per monomer, divided by k_BT, and as in Ohta and Kawasaki all energies will be divided by k_BT. From the interaction parameter χ, Ohta and Kawasaki define a new variable $\bar{\chi} = 2N_0\chi - s(f)/[2f^2(1-f)^2]$, where $s(f)$ is discussed below. From this and from $A(f) = 3/[N_0f^2(1-f)^2]$ and $B(f) = N_0/[4f(1-f)]$, the interfacial width $\xi = [B(f)/\bar{\chi}]^{1/2}$ is calculated and a ratio $\alpha = A(f)/B(f)$ defined. The interfacial tension is calculated to be $\sigma = 2^{3/2}\eta_e^2/(3\xi)$, where $\eta_e \approx {}^1/_2$.

As mentioned above, in order to obtain an analytical solution for the free energy, Ohta and Kawasaki used an approximation in three terms (their eq 3.19) for the vertex function Γ_q, where the inverse of $\Gamma_q^{-2}\chi/N_0$ is the structure factor of the star diblock:

$$\Gamma_q \approx [q^2N_0/2 + 6/q^2N_0f(1-f) + s(f)/f(1-f)]/[2N_0^2f(1-f)] \quad (4)$$

where the exact expression used for $s(f)$ did not affect their results. However, no value of $s(f)$ gives the correct asymptotic behavior for both $q \to 0$ and $q \to \infty$ simultaneously. In fact, as noted by Ohta and Kawasaki, even an average value of the two values of $s(f)$ dictated by these two limits produces a fit of the scattering curve that matches to only 4%.

The approach in this paper is to use the exact form of Γ_q given by de la Cruz and Sanchez, in which case the value of $s(f)$ that must be used is the value for the asymptotic behavior as $q \to \infty$:

$$\Gamma_q = \{q^2N_0/[4N_0^2f(1-f)]\}\{1 + 2s(f)/[q^2N_0f(1-f)]\} \quad \text{for } q \to \infty \quad (5)$$

where

$$s(f) = 1 - (n-1)(1-f)/2 + (n-3)f(1-f)/2 \quad (6)$$

With this, if one defines the function $\gamma(q)$ by subtracting the q^2 term and the term containing $s(f)$, i.e., via

$$\Gamma_q = \{q^2N_0/2 + 6\gamma(q)/[f(1-f)] + s(f)/[f(1-f)]\}/[2N_0^2f(1-f)] \quad (7)$$

then $\gamma(q) = 1/q^2N_0$ as $q \to 0$ and $\gamma(q)\Psi_{-q}$ is summable. The Ohta and Kawasaki approximation amounts to taking $\gamma(q) = 1/q^2N_0$. However, one can calculate that

$$\lim_{q\to\infty} \gamma(q)q^2N_0 = [2(n-1) - 3]/12 + [2 - (n-1)(1-f)]^2/[12f(1-f)] + (n-3)[2 - (n-1)(1-f)]/12 \quad (8)$$

With this form for Γ_q, the long-range contribution to the free energy can be written as

$$F_L\{\Psi\} = (\alpha/2)(2\eta_e)^2N_0\int\int\int \gamma(\mathbf{q})\Psi_q\Psi_{-q}\, d^3\mathbf{q} \quad (9)$$

Of course, the form factor of Ψ_q need only be calculated for the case when the lattice parameter $\chi = 1$; hence define $\Phi(q)$ to be the squared-norm of the form factor (or $\Psi_q\Psi_{-q}$) when $X = 1$. However, although it is approximately true that $\gamma(q)$ scales as X^2, we are not employing this approximation and therefore the X dependence of γ will be included in the computation. Specifically, this is done by writing $|\mathbf{q}|$ in its actual form as $q = 2\pi|(h,k,l)|/X$ and taking the argument of the Debye functions in the expression of de la Cruz and Sanchez (their eq 28) to be

$$X_0 = N_0q^2\lambda^2/6 \quad (10)$$

The statistical segmental length λ will be taken to be $3^{1/2}$, in the symmetric case. Because of the complicated X-dependence of $\gamma(q)$, it is necessary to solve iteratively for the value of X that minimizes the total free energy.

This total free energy is the sum of F_L and the interfacial tension term, eq 4.12 in Ohta and Kawasaki, which contains the q^2 term and the $s(f)$ terms that were subtracted from Γ_q, as well as the χ term. Define A_0 to be the interfacial area per unit volume when $X = 1$, and the expression for the total free energy is

$$F = \sigma A_0/X + (\alpha/2)(2\eta_e)^2N_0\sum\gamma(q)\Phi(q) \quad (11)$$

where the summation is over the reciprocal lattice vectors of the periodic structure. For direct comparison with Ohta and Kawasaki, we divide the free energies by Q where

$$Q = 2^{1/2}f(2^{1/2}\xi\alpha)^{1/3}/3 \quad (12)$$

If one factors out the η_e^2/ξ from the expression for F, the factor $\alpha\xi N_0$ appears in front of the second term. The parameter χN_0 appears in the formula for ξ through $\bar{\chi}$. The relation between $\alpha\xi N_0$ and χN_0 is given by

$$\alpha\xi N_0 = [A(f)N_0/B(f)][B(f)/\bar{\chi}]^{1/2} = A(f)N_0/[B(f)\bar{\chi}]^{1/2} \quad (13)$$

The final forms of the formulas involving $A(f)$ and χ have been written so as to emphasize the fact that $A(f)$ and χ appear only in the combinations $A(f)N_0$ and χN_0, which are independent of the statistical step length. The only dependencies on the polymer index in the final equations are those arising directly from the arguments of the Debye functions in Γ_q. Thus, for example, the factor $1/2c = N/2\rho_0$ in eq 3.14 of Ohta and Kawasaki, which would require a volume-weighted polymer index (as defined by Helfand,[24] e.g.), cancels out in the final formulas.

Before proceeding to the asymmetrical case, we consider the accuracy of the free energy calculation based on eq 11. By eq 2, $\Psi_q \sim 1/q^2$, so that $\Phi(q) \sim 1/q^4$ (a simple consequence of the assumption of sharp interfaces), and the number of terms at a radius of $\mathbf{q}$ in reciprocal space goes as q^2. Since by eq 8 $\gamma(q)N_0 \sim 1/q^2$, the sum in eq 11 has an upper bound that can be approximated by $\int_{2^{1/2}}1/q^4\, dq$, where without loss of generality we choose the lattice parameter to be such that the minimum wave vector is (1,1,0). In our calculations, all reciprocal lattice vectors of the form (h,k,l) where $-21 \le h,k,l \le 21$ were included in the sum. Thus the relative error can be estimated by the ratio $\int_{21}1/q^4\, dq/\int_{2^{1/2}}1/q^4\, dq = 0.03\%$ (actually this overestimates the error because lattice vectors such as (19,19,19), which have a reciprocal-space radius greater than 21, are included in our sum). Indeed, when $\gamma(q)$ was taken to be $1/q^2N_0$ as in the Ohta and Kawasaki approximation, our numerical sum differed from their analytical formulas by less than 0.03% in the case $n = 1$. Because the form factors for the OBDD structure are calculated analytically, the order of relative error in this sum is 0.03%. Furthermore, since the total free energy varies as the ${}^1/_3$ power of this sum, the relative error in the total free energies is very small and is in fact controlled mostly by the errors in surface areas calculated from the finite element solutions (the total free energy varies as the ${}^2/_3$ power of this area).

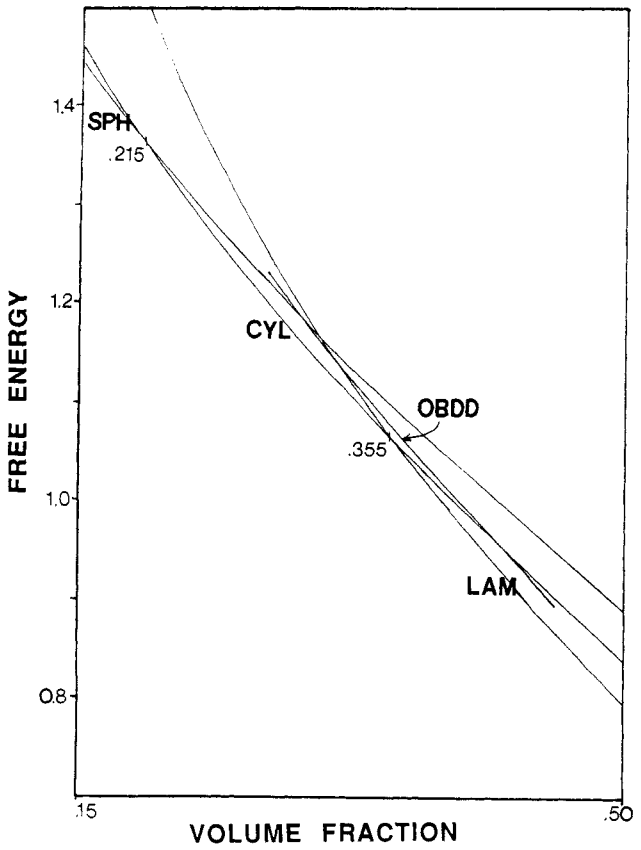

Figure 4. A plot of the free energy for various microdomain structures versus composition for the limit of strong segregation ($N_0\chi = 10^6$). Units of energy are as given by Ohta and Kawasaki.[11] The microdomain structural transitions between spheres and cylinders and cylinders and lamellae occur at $\phi = 0.215$ and 0.355, respectively.

This error in surface area is on the order of 0.05%.[15]

For the polymer indices normally encountered in experiments, the dependence of the relative free energies of the various morphologies on the segmental lengths and densities is negligible, and within the context of the present theory, the relative free energies given in Figure 4 hold for all molecular weights. However, we wish also to use the theory to interpret and predict experimentally measured *lattice* parameters, and for these purposes, as well as in cases where one or both polymers are very stiff with a small number of statistical segments per block, we would like to generalize the equations to incorporate the particular molecular parameters of the system in question. Let the statistical segmental lengths of the A and B blocks be λ_A and λ_B. These values together with the block molecular weights determine the radii of gyration of the A and B blocks, which we will call R_A and R_B. The arguments of the Debye functions in Γ_q become $R_A^2q^2$ (replacing fx) and $R_B^2q^2$ (replacing $(1-f)x$). To bring the nomenclature into coincidence with that of Ohta and Kawasaki, we take the unit of length u to be the Kuhn length of the B blocks divided by $3^{1/2}$ and define f by $f = R_A^2/(R_A^2 + R_B^2)$ and N_0 by $N_0 = 2(R_B/u)^2/(1-f) = 2(R_A/u)^2/f$. These definitions guarantee that $R_B^2 = (1-f)N_0\lambda_B^2/6 = (1-f)N_0u^2/2$ and $R_A^2 = fN_0\lambda_A^2/6 = nN_0u^2/2$, where in each case the first form is that of de la Cruz and Sanchez and the last form that of Ohta and Kawasaki when u is taken to be unity.

The prefactors in front of the Debye functions, which are f^2 and $(1-f)^2$ in the symmetric case, reflect the actual volume fractions ϕ_A and ϕ_B rather than the ratio expressed in the above equation for f, because the weighting of the scattering contributions must be according to the square of the volume fractions. Thus the expression for D_f in eq 28 of de la Cruz and Sanchez is $D_f = \phi_A^2D(fN_0q^2/2) = \phi_A^2D(R_A^2q^2)$ and similarly for D_{1-f}. Also the expression for F_f becomes $F_f = \phi_A[1 - \exp(-fN_0q^2/2)]/(fN_0q^2/2)$ and similarly for F_{1-f}.

By examining the limit of Γ_q with these definitions, the expression for $s(f)$ becomes

$$s(f) = [f(1-f)/2a^2b^2)]\{(n-1)a^2 + 2ab - 2(a^2+b^2) - [fa^2 + (1-f)b^2][(1-f)(n-1) - 2]/[f(1-f)]\} \quad (14)$$

where $a = \phi_A/f$ and $b = \phi_B/(1-f)$. And, finally, the leading $q^2N_0/2$ inside the brackets in eq 7 must be changed to

$$q^2N_0[fa^2 + (1-f)b^2]/(2a^2b^2) \quad (15)$$

4. Results

In the symmetric case, namely, $\lambda_A = \lambda_B$ and $\rho_{0A} = \rho_{0B}$, the sphere/cylinder and cylinder/lamellae crossover points remain within a few percentage points of the values given by Ohta and Kawasaki, that is, $\phi_1 = 0.215 \pm 0.02$ and $\Phi_2 = 0.355 \pm 0.02$, for a wide range of χ, N_0, and n. The OBDD morphology yields an energy that is at least 1% higher than the minumum of the other three energies. Figure 4 shows the free energies for linear diblocks ($n = 1$) in the strong segregation regime ($N_0\chi = 10^6$)—so that the energies for spheres, cylinders, and lamellae agree with those given by Ohta and Kawasaki—and although the OBDD energy is competitive with that of the other three morphologies, it is never the smallest.

In the general case, where the segmental lengths and densities are not necessarily the same, the N_0 dependence of the lattice parameter is very close to the $^2/_3$ power law given by Ohta and Kawasaki and observed in many experiments (e.g., Hashimoto et al.,[25] Alward,[3] and Mori et al.[17]). The dependence on the parameter χ, and hence on the inverse of temperature, is also very much as in the theory of Ohta and Kawasaki. Both of these dependencies can be expressed by the fact that X scales as $(\alpha\xi)^{-1/3}$, via the equation for $\alpha\xi$ given above; for sufficiently large χN_0 ($\gg s(f)$, it is seen that $\alpha\xi$ scales as N_0^{-2} and as $\chi^{-1/2}$, yielding $X \sim N_0^{2/3}$ and $\chi^{1/6}$. This $^{-1}/_3$ power dependence on $\alpha\xi$ was stated in different but equivalent terms by Ohta and Kawasaki, namely, as $X \sim \xi^{-1/3}R_g^{4/3}$, where $R_g \sim \alpha^{-1/4}$. The scaling $X \sim (\alpha\xi)^{-1/3}$ follows easily upon noting that the long-range term containing the factor $\alpha\xi$ goes very nearly as X^2, whereas the short-range term goes as $1/X$. It should be noted that the scaling with χN_0 is much more dependent on the assumption of large N_0 than is the scaling with $\alpha\xi$, because of term involving $s(f)$ in the denominator of eq 13.

In the comparison of the theory with experiments on PI/PS star and linear diblocks that follows, the dimensionless lattice parameter X has been made dimensional by multiplying by the unit of length, which, as stated above, is the outer (B) block segmental length divided by $3^{1/2}$. The value of the characteristic ratio for PS is approximately 12.4,[26] so $\lambda_B = 19.1$ Å. The characteristic ratio of PI is approximately 6.4, so $\lambda_A = 9.9$ Å. The value of χ was that determined by Mori et al.[17] using SAXS. The value of χ used here will be the value extrapolated to 115 °C from the data of Mori et al, with their formula $\chi = -0.0937 + 66/T$, namely, $\chi = 0.076$. These values of χ and λ determine all the inputs to the present theory, and no adjustable parameters remain.

The comparison of the theory with experimental data will now be given for the case involving the OBDD structure that has been most closely examined. This was the case[16,3] of star copolymers of 10000 MW PS outer

Table II[a]
Lattice Parameters and Free Energies: Cylinder and OBDD Star Diblocks

no.	obsd morph	X_{exptl}, Å	X_{theor}, Å	F_{OBDD}	F_{Lam}	F_{cyl}	F_{OBDD}/F_{cyl}
2	cyl	225[b]	231	1.156	1.173	1.132	1.0225
4	cyl	225[b]	237	1.095	1.116	1.067	1.0264
5	cyl	245	237	1.083	1.105	1.054	1.0276
6	OBDD	365	355	1.083	1.100	1.048	1.0283
8	OBDD	340	354	1.070	1.107	1.049	1.0288
12	OBDD	345	351	1.105	1.127	1.075	1.0279
18	OBDD	350	348	1.169	1.191	1.140	1.0255

[a] Comparison of theory with experimental data of Alward et al.[3] For each arm number listed, the observed morphology and the lattice parameter from SAXS are listed, followed by the theoretically calculated lattice parameter for the observed morphology and the total calculated free energies for the candidate morphologies. Units of energy are as in Ohta and Kawasaki. [b] The values originally cited in Alward et al.[3] for these two samples are in error.

blocks, 23 000 MW PI inner blocks, and arm numbers of two, four, five, six, eight, 12, and 18. SAXS was used to determine the lattice parameters and, together with TEM, the morphology. These are summarized in Table II giving the (10) spacing (in angstroms) for cylindrical morphologies and the $Pn3m$ lattice parameter for the OBDD structures. Table II gives the results of the free energy and lattice parameter calculations from the H-surface model. It can be seen that the predicted lattice parameters for the OBDD morphology are in excellent agreement with values measured in the samples which exhibit the OBDD morphology. It should be noted that the measured values in all four OBDD structures are the same within the experimental error, so that no conclusions can be made concerning variation with arm number. Concerning the free energy competition, the theory fails to predict a favorable free energy for the OBDD over that of the cylindrical morphology at higher arm numbers, as indicated by the experiments. In the next section we argue that this is due mainly to the failure in the theory, inherent to the Gaussian approximation, to account for the conformational changes near the star center due to crowding. Nevertheless, the OBDD free energies are still lower than those for the lamellar morphology (and also the BCC sphere morphologies, which are not shown because the energies are not competitive in this composition range), and the overall trend of the OBDD free energy being lower than that of lamellar and competitive with that of cylinders, at volume fractions corresponding to the area minimum in Figure 1b, is consistent with the compositional dependence of the OBDD morphology observed by Herman et al.[7]

Another comparison of the theory with experiments can be made with the data of Hasegawa et al.[8] in which the OBDD was apparently observed in three high MW PI/PS *linear* diblocks. While the published electron micrographs strongly indicate the OBDD morphology, the SAXS data are more consistent with the cylindrical morphology, according to those authors. Table III gives the calculated total free energies at these three compositions. The very small difference—about 1% in all three cases—between the cylindrical and OBDD free energies suggests that both types of structure might coexist in a metastable state. In Table III are also listed the experimentally measured lattice parameters and the calculated predictions for the experimentally observed morphology. Given the error involved in estimating the lattice parameter from electron micrographs of stained, microtomed sections, the agreement with the theoretical lattice parameters is fairly good.

One result of our calculations that can be tested experimentally is that, for PI inner block, PS outer block

Table III[a]
Lattice Parameters and Free Energies: OBDD Linear Diblocks

PS vol fract	total MW	X_{exp}, Å	X_{theor}, Å	F_{OBDD}	F_{Lam}	F_{cyl}	F_{OBDD}/F_{min}
0.62	95 600	830	700	1.1738	1.1593	1.1635	1.0125
0.66	186 000	1230	990	1.1780	1.1650	1.1670	1.0112
0.63	207 000	1430	1068	1.1515	1.1364	1.1423	1.0133

[a] Comparison of theory with experimental data of Hasegawa et al.[8] The lattice parameters from TEM are listed, followed by the theoretically calculated OBDD lattice parameter and the total calculated free energies for the candidate morphologies. Units of energy are as in Ohta and Kawasaki. The energies for the bcc spheres are much higher at these compositions and are not included.

stars at the same arm molecular weight of 33 000, the PS-rich side of the phase diagram is predicted to exhibit OBDD morphologies for high arm numbers only. Calculations of free energies for a PI volume fraction of 0.27 show that while the free energy of the OBDD is higher than that of cylinders by more than 2.5% for arm numbers less than six, this difference becomes approximately 0.5% for an arm number of 18. Very few samples have been examined on the PS-rich side of the phase diagram for arm numbers this high, so that thus far, there has been no report of an OBDD morphology for a star with an inner block volume fraction less than 0.5 Presently work is in progress in this laboratory to check this composition range carefully.

The smallest volume fraction observed thus far in experiments for the phase occupying the diamond network is 0.27. Furthermore, this volume fraction in all the cases observed has been between 0.27 and 0.38. This is in perfect agreement with the present theory, because the lowest OBDD free energies occur for the structures near the minimum in surface area in Figure 1b, where as mentioned above this minimum also represents the structure with the lowest diamond-network volume fraction (0.262) in this family. The question of whether or not there exist other families of surfaces with this same topology and space group, but lower volume fractions, is discussed in ref 15 and is also the subject of present investigations by this group and elsewhere.

5. Discussion

We have made attempts to use electron microscopy data directly to determine the shape of the C/M interface and to estimate the extent of the shape fluctuations. An electron micrograph of a 12-arm PS/PI OBDD sample was digitized, and a computer was used to simulate the micrographs by sending rays through the 3D theoretical structure and calculating the resulting 2D projection gray level at each pixel (94 × 94 pixels). The details of the projection calculation will be given in a forthcoming publication (Anderson et al.[27]). The right half of part a of Figure 5, and of part b, is a theoretical projection using the constant-mean-curvature model. The left half of Figure 5a is the digitized experimental micrograph. The left half of Figure 5b is the data after restoration with a maximum entropy algorithm which is applied iteratively on the real image and on the power spectrum of the image.[28] Considerable symmetrization has been accomplished by the algorithm, in a well-defined manner totally free from any user bias. An error measure has been defined as the L_2 norm of the difference between the calculated and measured grey levels, normalized to the L_2 norm expected for a random grey-level map. The normalized error between the calculated and experimental grey levels before

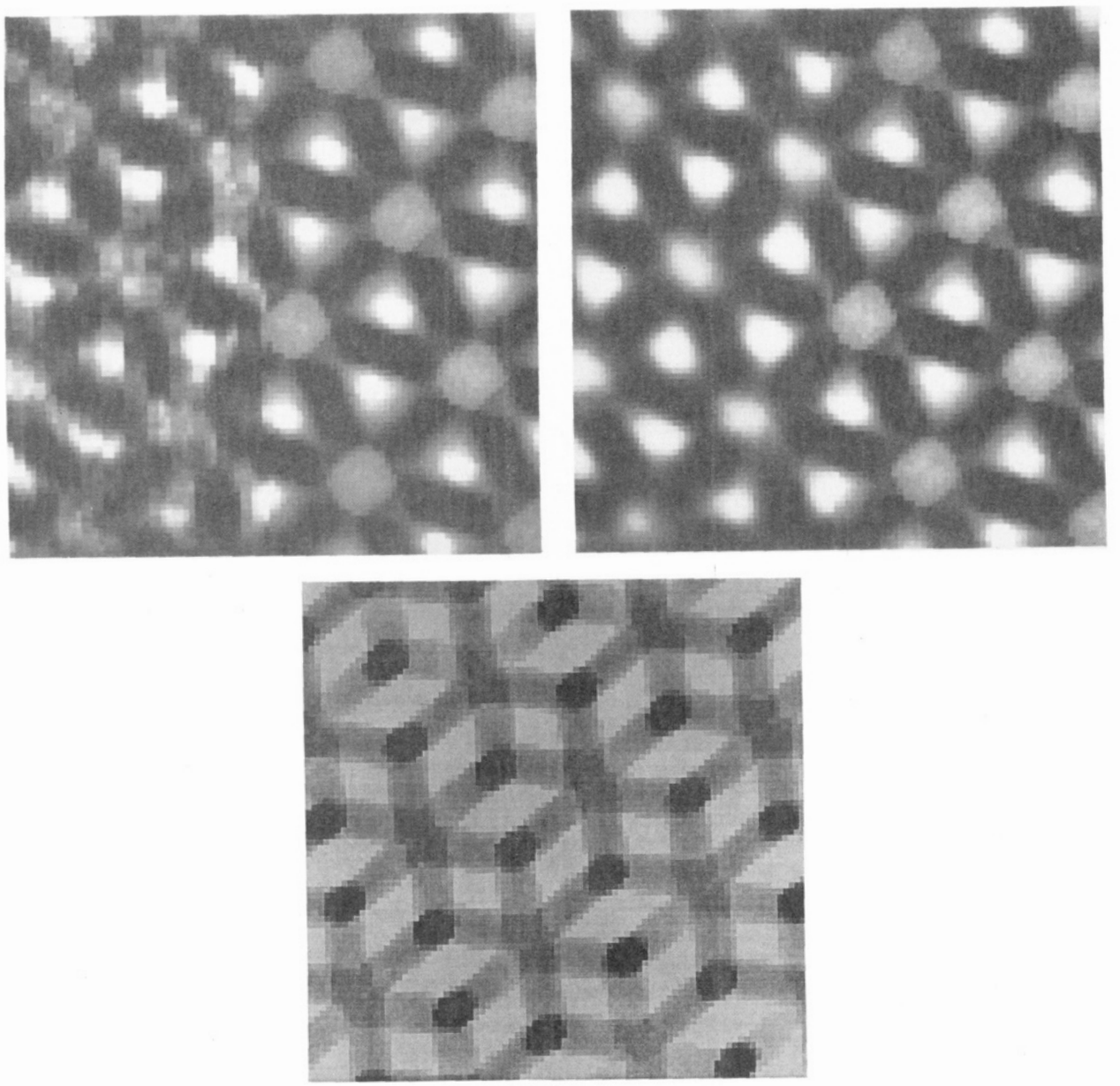

Figure 5. (a, Top left) Digitized bright field TEM image (left half) of the microdomain morphology of a 12-arm PS/PI star diblock copolymer alongside the computer-simulated projection (right half) of the model structure whose PS/PI interface is Figure 2. The projection is approximately [111] and the volume fraction of the PS phase (light regions) is 0.27. (b, Top right) Digitized bright field TEM image (left half) after restoration with a maximum entropy algorithm alongside the computer-simulated projection (right half). (c, Bottom) Computer-simulated projection of a model structure made of tetrahedrally joined cylindrical struts. In this model, the PS/PI dividing surface is a constant distance away from the two diamond graphs shown in Figure 2.

restoration is 0.395. The normalized error after restoration—Figure 5b—is considerably smaller, 0.295. The match between model and experiment in Figure 5b is remarkable. In Figure 5c we show the simulated image calculated when the cylindrical-strut model of the interfacial shape is used, and the match is quantitatively and even qualitatively poorer than when the constant-mean-curvature surface is used. The surface parallel to the minimal surface model is almost indistinguishable on this basis alone from the constant-mean-curvature surface model. However, these data combined with the data in Table I provide strong evidence that the dividing surface is best represented by the surface of constant mean curvature—as in the other classical microdomain morphologies.

Although the free energy comparisons in Table I involve very slight energy differences, we nevertheless believe they are meaningful because we are comparing morphologies of the same symmetry and topological type, and the results are easily interpreted in terms of interfacial surface area and chain conformations. However, when comparing free energies between morphologies of different symmetry and topology, the approximations going into the model thermodynamic potential do not cancel out and small energy differences between candidate structures cannot be taken too seriously. Moreover, the theoretical approach we have followed is based on Gaussian chain statistics. One knows that this assumption is inadequate on two grounds: (i) the structural dimensions in the microphase-separated state scale as $N_0^{2/3}$, and (ii) for star molecules, the core effects the inner-block chain conformations. The effect of the core on the chain conformations of the inner blocks has been recently observed in Monte Carlo simulations[29] and treated by a conformation space renormalization group (RG)

theory.[30] As mentioned above, the chain conformational statistics derived by renormalization group calculations on star copolymers have not yet been incorporated into a calculation of Γ_q that would more accurately reflect the core effect. Alward[16] believed the arm number dependence of the star diblock morphology was due to the core effect. But a simple modification to the present theory attempting to incorporate some of the results of the RG theory failed to account for this dependence. We now describe this modification.

The mean-square distance of the segments in a star polymer from the star center have been derived by Miyake and Freed[30] as a function of arm number and, most importantly here, a parameter ζ, where $\zeta = 0$ corresponds to the Gaussian chain statistics limit and $\zeta \to \infty$ corresponds to the fully developed excluded-volume limit. Therefore the ratio

$$\Omega^2 = \langle R^2 \rangle_\zeta / \lim_{\zeta \to 0} \langle R^2 \rangle_\zeta = 1 - (\zeta/(1+\zeta))[7/12 + (n-1)(13/12 - 2 \ln 2)]/4 \quad (16)$$

gives the increase in the mean-square distance of an A segment from the star center due to the crowding near the core, as a function of ζ and n. Our modification consists of changing the radius of gyration of the inner blocks in the Debye functions above to reflect this increase. Note that it is rather artificial to maintain the assumption of Gaussian statistics (in the Hamiltonian), while using the value for the increase in the radius of gyration that is due to a deviation from Gausian statistics. However, in lieu of a structure factor calculation based on the RG statistics, we know of no other tractable way to incorporate the core effect in this theory.

The results of the theory when the Ω factor is introduced do not compare well with the experimental results of Thomas et al.[2] While the free energy of the OBDD morphology becomes more favorable with respect to that of cylinders, the predicted lattice parameters become much higher than the experimental value long before the OBDD free energy becomes comparable to (within 1% of, say) that of cylinders.

Conclusions

The theory of Ohta and Kawasaki for the strong-segregation limit of linear diblock copolymers has been extended to star diblocks, with the inclusion of the newly discovered "ordered bicontinuous double-diamond" morphology. A thermodynamic potential has been defined that is a function of arm number, composition, interaction parameter χ, radii of gyration of the two blocks, and morphology. Calculation of this free energy requires the structure factor of the star diblock, which is used in the form as calculated by de la Cruz and Sanchez. A numerical summation over 2000 reciprocal lattice vectors yields an accuracy of better than 0.05% under the assumptions of the model, the most important of which are the random-phase approximation of de Gennes and the model Hamiltonian. There are no free parameters in the model.

The major results of the calculation which are not included in the results of Ohta and Kawasaki can be summarized as follows:

(1) The OBDD morphology becomes most competitive with the other morphologies at volume fraction ϕ_C:ϕ_M ratios just above 0.26:0.74, corresponding to the minimum in surface area in the family of constant-mean-curvature dividing surfaces of OBDD symmetry and topology.

(2) Both free energy calculations and comparisons of theoretical model projections with TEM data indicate that the dividing surface between the PI and PS phases is of constant mean curvature.

(3) The present theory cannot account for the transition from the cylindrical morphology to OBDD with increasing arm number, possibly because it does not include the effect of the crowding near the core on chain conformations.

(4) It is nevertheless possible to make accurate predictions of lattice parameters by using the theory.

Presently, work is in progress to use the approach of Helfand and Wasserman[31] to model the free energies, where this approach should have more success in taking account of the non-Gaussian conformations of star molecules.

It should be mentioned that the present approach can be easily modified to treat simple graft copolymers and A_nB_n stars, the structure factors of which were calculated by de la Cruz and Sanchez. This has not been done here, however, because at present the authors know of no documented experiments on these types of copolymers. Efforts are under way in our group to examine A_nB_n stars.

As a final remark, because the study of the morphology of star copolymers is in its infancy, there is always the possibility that other structures will be found to occur as equilibrium morphologies. For example, in surfactant systems, microstructures based on the Schwarz "P" minimal surface[4] of primitive cubic symmetry (e.g., Lindblom et al.[32]) and related H-surfaces [15], the "gyroid"[18] minimal surface (e.g., Hyde et al.[33]), and H-surfaces of the "I-WP" family[15] have been discovered. Furthermore, these structures have been shown to bear a close relationship to simple close packings of spheres[15], and have significantly lower surface areas than these sphere packings. The subject becomes even richer when one considers the structures that appear in transitions between known structures, at grain boundaries, and in thin films.[34]

Acknowledgment. Financial support from the University of Massachusetts Institute for Interface Science (supported by IBM), the National Science Foundation, Grant DMR 84-06079, and the Applied Mathematical Sciences Subprogram of the Office of Energy Research, U.S. Department of Energy, is gratefully acknowledged. The authors would also like to thank Profs. M. Muthukumar and M. Olvera de la Cruz and Dr. Glenn Fredrickson for valuable discussions.

Registry No. (S)(I) (block copolymer), 105729-79-1.

References and Notes

(1) Bi, L, K.; Fetters, L. J. *Macromolecules* **1976**, *9*, 732.
(2) Thomas, E. L.; Alward, D. B.; Kinning, D. J.; Martin, D. C.; Handlin, D. L, Jr.; Fetters, L. J. *Macromolecules* **1986**, *19*(8), 2197.
(3) Alward, D. B.; Kinning, D. J.; Thomas, E. L.; Fetters, L. J. *Macromolecules* **1986**, *19*, 215.
(4) Schwarz, H. A. *Gesammelte Mathematische Abhundlungen*; Springer: Berlin, 1890; 2 volumes.
(5) Scriven, L. E. *Nature (London)* **1976**, *263*, 123. See also: Scriven, L. E. In *Micellization, Solubilization, and Microemulsions*; Mittal, K. L., Ed.; Plenum: New York, 1977; Vol. 2, p 877.
(6) Kinning, D. J.; Alward, D. B.; Thomas, E. L.; Fetters, L. J. *Macromolecules* **1986**, *19*, 1288.
(7) Herman, D.; Kinning, D. J.; Fetters, L. J.; Thomas, E. L. *Macromolecules* **1987**, *20*, 2940.
(8) Hasegawa, H.; Tanaka, H.; Yamasaki, K.; Hashimoto, T. *Macromolecules* **1987**, *20*, 1651.
(9) Kinning, D. J.; Ottino, J. M.; Thomas, E. L. *Macromolecules* **1987**, *20*, 1129.
(10) Leibler, L. *Macromolecules* **1980**, *13*, 1602.
(11) Ohta, T.; Kawasaki, K. *Macromolecules* **1986**, *19*, 2621.
(12) Fredrickson, G. H.; Helfand, E. *J. Chem. Phys.* **1987**, *87*(1), 697.
(13) de la Cruz, M. O.; Sanchez, I. C. *Macromolecules* **1986**, *19*, 2501.

(14) Helfand, E.; Sapse, A. M. *J. Chem. Phys.* **1975**, *62*(4), 1327.
(15) Anderson, D. M. Ph.D. Dissertation, University of Minnesota, Minneapolis, MN, 1986.
(16) Alward, D. B. Ph.D. Dissertation, University of Massachusetts, Amherst, MA, 1984.
(17) Mori, K.; Hasegawa, H.; Hashimoto, T. *Polym. J. (Tokyo)* 1985, *17*, 799.
(18) Schoen, A. *NASA Tech. Note* **1970**, *TN D-5541*.
(19) Nitsche, J. C. C. *Arch. Rat. Mech. Anal.* **1985**, *89*, 1.
(20) Anderson, D. M.; Leibler, S.; Gruner, S. *Proc. Natl. Acad. Sci. U.S.A.*, in press.
(21) Hosemann, R.; Bagchi, N. *Direct Analysis of Diffraction by Matter*; North-Holland: Amsterdam, 1962.
(22) Mackay, A. L. *Nature (London)* 1985, *314*, 604.
(23) Karcher, H., in preparation.
(24) Helfand, E. *Macromolecules* **1975**, *8*, 552.
(25) Hashimoto, T.; Shibayama, M.; Kawai, H. *Macromolecules* **1980**, *13*, 1237; *16*, 1093. Also: Hashimoto, T.; Fujimura, M.; Kawai, H. *Macromolecules* **1980**, *13*, 1660.
(26) Brandrup, J. Immergut, E. H. Eds. *Polymer Handbook*; Wiley: New York, 1975.
(27) Anderson, D. M.; Thomas, E. L.; Hoffman, J.; Hoffmann, D., to be submitted for publication.
(28) Anderson, D. M.; Martin, D. C.; Thomas, E. L., submitted for publication in *Acta Crystallogr., Sect. A.*
(29) Mattice, W. L. *Macromolecules* **1984**, *17*, 415.
(30) Miyake, A.; Freed, K. F. *Macromolecules* **1984**, *17*, 678.
(31) Helfand, E.; Wasserman, Z. R. *Macromolecules* **1976**, *9*, 879. *Ibid.* **1978**, *11*, 960.
(32) Lindblom, G.; Larsson, K.; Johansson, L.; Fontell, K.; Forsen, S. *J. Am. Chem. Soc.* **1979**, *101*, 5465. See also: Fontell, K.; Lindman, H.; *J. Phys. Chem.* **1983**, *87*, 3289.
(33) Hyde, S.; Anderssen, T.; Ericsson, J. Larrson, K. *Z. Kristallogr.* **1984**, *168*, 213.
(34) Thomas, E. L.; Anderson, D. M.; Henkee, C.; Hoffman, D. *Nature (London)* **1988**, *334*, 598-601.

Conformational Characteristics of Polyesters Based on Terephthalic Acid with an Ether Group in the Glycol Residue

César C. González, Evaristo Riande,* Antonio Bello, and José M. Pereña

Instituto de Ciencia y Tecnologia de Polimeros (CSIC), Juan de la Cierva, 3, 28006 Madrid, Spain. *Received February 24, 1988; Revised Manuscript Received April 22, 1988*

ABSTRACT: Poly(ditrimethylene glycol terephthalate), prepared by the melt-phase procedure from dimethyl terephthalate and ditrimethylene glycol, was studied with regard to its unperturbed dimensions and polarity. From viscometric and osmotic results obtained in tetrahydrofuran solutions, the unperturbed dimensions ratio $\langle r^2\rangle_0/M$, where $\langle r^2\rangle_0$ is the mean-square end-to-end distance in the unperturbed state and M the molecular weight, was found to be ca. 0.90 Å^2 mol g^{-1} at 30 °C. From dielectric measurements carried out on benzene solutions the mean-square dipole moment of the chains was determined; this quantity, expressed in terms of the dipole moment ratio $\langle\mu^2\rangle/n\mu^2$, where $n\mu^2$ is the mean-square dipole moment of the chain in the idealization that all the skeletal bonds are freely jointed, amounts to ca. 0.80 at 30 °C and it exhibits a slightly negative temperature dependence. Both the unperturbed dimensions and the dipole moments were interpreted by using the rotational isomeric state model. The principal conclusion of this analysis is that these conformational properties are extremely dependent on the gauche population about CH_2–CH_2 bonds of the glycol residue and the dimensions are also very sensitive to the second-order interactions arising from gauche rotations of different sign about two consecutive CH_2–CH_2 skeletal bonds. Stabilizing gauche effects about CH_2–CH_2 bonds reported in poly(trimethylene oxide) were not detected in the present system.

Introduction

The configuration-dependent properties of polyesters with repeating unit $OOCC_6H_4COO(CH_2)_n$ are strongly dependent not only on the number of methylene groups of the glycol residue but also on the nature of the acid (terephthalic, isophthalic, or phthalic) residue. In polyesters based respectively on terephthalic and isotphthalic acids, coplanarity between the carbonyl and phenyl groups guarantees maximum overlapping of electrons of these groups[1] and consequently the rotational angles about C^{Ph}–CO bonds are restricted to 0 and 180°.[2] The planar conformation of the terephthaloyl and isophthaloyl residues favors the molecular packing of the chain in the crystal and enhances the attractive intermolecular interactions between the ester groups of neighboring chains. As a result, the polyesters exhibit high melting points whose values decrease as the number of methylene groups in the glycol residue increases,[3] reaching a minimum, and then increase eventually reaching the T_m of polyethylene for $n \to \infty$. In contrast, large repulsive intramolecular interactions between two ester groups of the phthaloyl residue overcome the stabilizing effects of the coplanarity between the carbonyl and phenyl groups and the critical interpretation of conformation-dependent properties of polyesters based on phthalic acid[4] suggests that the rotational angles about C^{Ph}–CO bonds are ±90°. Consequently, the molecular packing of the chains in the crystal seems to be disfavored, hindering the possibility that crystallinity is developed in phthalate-based polyesters in which the number of methylene groups in the glycol residue is small.

The structure of the glycol residue also has a big effect on the physical properties of polyesters based in aromatic diacids, and this work is part of a more general investigation dealing with the influence of ether glycol residues on the conformational properties of polyesters based on aromatic diacids, specifically, on terephthalic acid.[5-10] Results have been reported that indicate that poly(diethylene glycol terephthalate) (PDET) hardly crystallizes from the bulk and only crystallizes from dilute solutions.[7] The closeness of the glass-transition temperature (~20 °C) to the melting temperature (~90 °C) in PDET seems to enhance the transport term in the crystallization process, slowing down the development of crystallinity in the bulk polymer. An important conformational characteristic of PDET is that gauche states about CH_2–CH_2 bonds of the glycol residue are 0.8 kcal mol^{-1} below that of the alternative trans state.[11] It seems that the presence of neighboring carbonyl groups enhances the gauche population about CH_2–CH_2 bonds with respect to that of similar bonds in poly(ethylene oxide) (PEO) where gauche states about

0024-9297/88/2221-3230$01.50/0